1996A&A...312..463P

Astron. Astrophys. 312, 463–474 (1996)

ASTRONOMY AND ASTROPHYSICS

Pulsation models of δ Scuti variables

I. The high-amplitude double-mode stars

J.O. Petersen[1] **and J. Christensen-Dalsgaard**[2]

[1] Theoretical Astrophysics Center, and Niels Bohr Institute for Astronomy, Physics and Geophysics, Astronomical Observatory, Øster Voldgade 3, DK-1350 Copenhagen K, Denmark (oz@astro.ku.dk)
[2] Theoretical Astrophysics Center, and Institute of Physics and Astronomy, Aarhus University, DK-8000 Aarhus C, Denmark (jcd@obs.aau.dk)

Received 20 October 1995 / Accepted 26 January 1996

Abstract. The relations between high-amplitude δ Scuti stars and the much more abundant low-amplitude δ Sct variables are not clear. Both groups have similar periods and seem to have almost the same basic physical properties, although their light-curve characteristics are very different. In the last few years much improved observational data have been published, and improved theoretical physics – in particular the new OPAL/OP opacities – now allows much more accurate calculations of theoretical evolution models including the normal–mode pulsation frequencies.

We here use new series of stellar envelope models to give calibrations of the first overtone–to–fundamental mode and the second–to–first overtone period ratios in terms of the primary model parameters: metal content and mass-luminosity relation. Effects of the secondary model parameters: hydrogen content, position within the instability strip and assumed efficiency of convection are also studied in detail, and shown to be small.

These results combined with pulsation analysis of new stellar evolution models are applied to discuss the available information for double-mode high-amplitude δ Sct stars. We conclude that observed period ratios and positions in the HR-diagram are in agreement with the assumption that these variables are normal stars following standard evolution.

Observational data for SX Phoenicis and AI Velorum are compared with theoretical evolution sequences. It is shown that the photometry and the observed two periods of SX Phe constrain the metal content to $Z = 0.001$, the mass to 1.0 solar masses and the bolometric magnitude to about 2.70 mag. The inferred distance of SX Phe gives a parallax of 0.012 ± 0.002 arcsec compared with that of the HIPPARCOS Input Catalogue of 0.023 ± 0.008 arcsec. For AI Vel the available photometry and the two primary observed periods do not provide a unique solution. Models based on OPAL opacities allow $Z = 0.01 - 0.02$ with corresponding masses $1.6 - 2.0$ solar masses. This can be understood by the compensating effects from Z and the mass-luminosity relation in the calibration of the period ratio. It is suggested that the surprisingly narrow interval in the first overtone–to–fundamental mode period ratio observed in the double-mode δ Sct stars may be due to these compensating effects. Attempting to fit low-amplitude modes observed in AI Vel in addition to the primary oscillations, it is concluded that the present models cannot explain these oscillations in terms of radial modes.

The little understood relations between high- and low-amplitude δ Sct stars are briefly discussed, and the problem of mode identification is emphasized.

Key words: stars: oscillations – stars: cepheids – stars: δ Sct – stars: individual: SX Phe – stars: individual: AI Vel

1. Introduction

The δ Scuti class of pulsation variable stars contains several interesting subgroups each with more or less peculiar unsolved problems, and the relation between the high-amplitude δ Scuti stars (HADS in the following) and the much more abundant low-amplitude δ Sct variables (LADS in the following) is not clear. Both groups have similar periods and seem to have almost the same basic physical properties, although their light-curve characteristics are very different. HADS typically have amplitudes of about 0.4 mag in V and oscillate in one or two stable frequencies, while the "normal" δ Sct stars (LADS) usually have amplitudes smaller than about 0.05 mag and oscillate in several frequencies simultaneously, showing a very complicated oscillation pattern.

We note that the high-amplitude δ Sct stars have also been denoted *dwarf Cepheids, AI Velorum stars,* and *RRs variables* in the literature. In recent years, the important Population II subgroup of low metallicity has been designated *SX Phoenicis* stars, after the prototype, and many have been found in globular clusters (e.g. Nemec & Mateo 1990). An interesting problem for

Send offprint requests to: J.O. Petersen

© European Southern Observatory • Provided by the NASA Astrophysics Data System

1996A&A...312..463P

these Population II variables is that such stars seem to be much younger and much heavier than allowed in standard evolution scenarios of the Galaxy. They belong to the "blue stragglers", which may be formed as a consequence of mass transfer in binary systems.

After the review papers by Baglin et al. (1973) and Breger (1979, 1980) the general consensus has been that *all* δ Sct stars (probably) are normal stars evolving according to standard stellar-evolution theory in the main-sequence or the immediate post–main–sequence stages. However, observational proof of the validity of this hypothesis is still missing. The best evidence until now is the presence of LADS in galactic clusters (e.g. Frandsen & Kjeldsen 1990) and of SX Phe stars in globular clusters with known distance (e.g. Nemec & Mateo 1990). In both cases the variables seem to be best explained by the standard evolution scenario. HIPPARCOS parallaxes will be important in this context. In particular, HIPPARCOS is expected to provide an accurate parallax of the field HADS SX Phe itself. Several attempts to provide more direct evidence on the nature of HADS, e.g. by determination of Wesselink-type radii (e.g. Fernley et al. 1987) have been made, usually with inconclusive results.

The crucial test of the nature of these stars is an independent, accurate and reliable mass determination, since alternative (and more speculative) possibilities proposed in the literature all predict much lower masses than the 1.0–2.5 solar masses obtained in the standard scenario (e.g. Petersen 1976). The generally accepted mass for an old evolved star is 0.6–0.8 solar masses, and masses of 0.2–0.3 solar masses have been suggested in the evolution of a component of a binary system proposed by Dziembowski & Kozłowski (1974). Interest in the low-mass possibility has increased recently due to the observational determination of several negative period derivatives, which give difficulties for the high-mass standard evolution scenario (e.g. Breger 1990; Rodríguez et al. 1995).

Before the OPAL/OP opacities became available (Iglesias et al. 1992), theoretical pulsation periods, and in particular period ratios, could not be relied upon, neither for classical Cepheids nor for δ Sct stars (e.g. Andreasen & Petersen 1988; Moskalik et al. 1992; Christensen-Dalsgaard 1993). Christensen-Dalsgaard & Petersen (1995) used the new opacities for a discussion of double-mode Cepheids in the Galaxy and the Large Magellanic Cloud. This analysis indicates that theoretical period ratios are now accurate within ± 0.001, a factor of 10 better than before 1992. In the present paper we use basically the same approach to discuss the double-mode high-amplitude δ Scuti variables, considering these stars as "dwarf Cepheids", thereby obtaining new constraints on the models from the accurate observed period ratios.

In Sect. 2 we describe the construction of evolution model sequences and envelope model series, and also comment on calculation of pulsation periods and their accuracy. The purpose of Sect. 3 is to provide an overview of pulsation periods and period ratios of δ Sct models. In particular, we discuss in some detail the Π_1/Π_0 (first overtone–to–fundamental mode) period ratio, because this ratio is known with high accuracy for several variable stars. We analyse the sensitivity of the period ratio to a number of model parameters. Π_2/Π_1 (second–to–first overtone period ratio) is also briefly discussed. In Sect. 4 we discuss the unique field HADS SX Phe itself in relation to the HIPPARCOS parallax to be released in 1996. AI Vel, which is unique among the HADS in having five reliably determined oscillation frequencies, is investigated by detailed modelling in Sect. 5, and other Population I variables are also briefly considered. Finally, Sect. 6 gives a short discussion emphasizing the high-amplitude group as a bridge between the classical Cepheids and "normal" δ Sct variables and summarizes our conclusions.

2. Stellar model series and pulsation calculations

In calculations of stellar envelope models the global parameters must be specified. We use the luminosity, L, as basic parameter in each model series, and specify mass-luminosity and radius-luminosity relations. In recent investigations of pulsation properties of classical Cepheids the problem of the relevant mass-luminosity relation has played a prominent role (e.g. Chiosi et al. 1993; Simon & Kanbur 1994; Christensen-Dalsgaard & Petersen 1995). The main reason is that the effect of overshooting on the luminosity in the Cepheid evolution stage is rather uncertain. This uncertainty can be parametrized by considering different mass-luminosity relations. We show in the following that realistic envelope models of δ Sct stars can be constructed as a continuation of standard Cepheid model sequences. Thus we use precisely the same parametrization as did Christensen-Dalsgaard & Petersen (1995) in the Cepheid case, starting from the the standard BIT-relation (Becker et al. 1977).

Although envelope models provide a convenient method for testing the sensitivity of the oscillation properties to the parameters of the stars, the procedure introduces some arbitrariness in the calculations. In studies of stars on or just after the central hydrogen-burning main sequence it might seem more natural to base the work on evolution sequences, especially when very accurate period ratios are required. Thus in the following we also consider results based on full evolution calculations and compare them with, for example, the BIT relation in the instability strip. In particular, evolution models are employed in Sects. 4 and 5 in the discussion of the observations of SX Phe and AI Vel.

2.1. Mass-luminosity relations of envelope models

Our envelope models are characterized by mass-luminosity relations of the form

$$\log M = A + B \log L \,, \tag{1}$$

with M and L in solar units. Table 1 summarizes the five relations used. ML1 is based on the standard BIT mass-luminosity relation for composition $(X, Z) = (0.70, 0.02)$ (Becker et al. 1977), while ML2 approximately fits calculations including a moderate amount of overshooting from convective cores (Chiosi et al. 1993). ML3 and ML4 are the relations suggested by Simon

© European Southern Observatory • Provided by the NASA Astrophysics Data System

1996A&A...312..463P

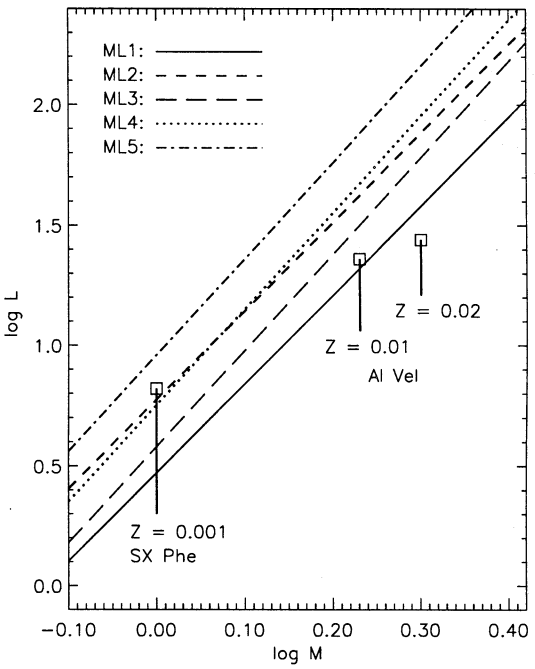

Fig. 1. Five mass-luminosity relations ML1–ML5 (cf. Table 1) in the ($\log M$, $\log L$) diagram. Vertical lines are evolution lines of models for SX Phoenicis and AI Velorum according to the analysis of Sects. 4 and 5 below, with the present positions (see text) marked by squares. Note that the present mass-luminosity ratio of AI Vel for Population I metal content, $Z = 0.01$, is close to ML1, while the position of the metal poor SX Phe is close to ML2 and ML4. This justifies our choice of $M - L$ relations

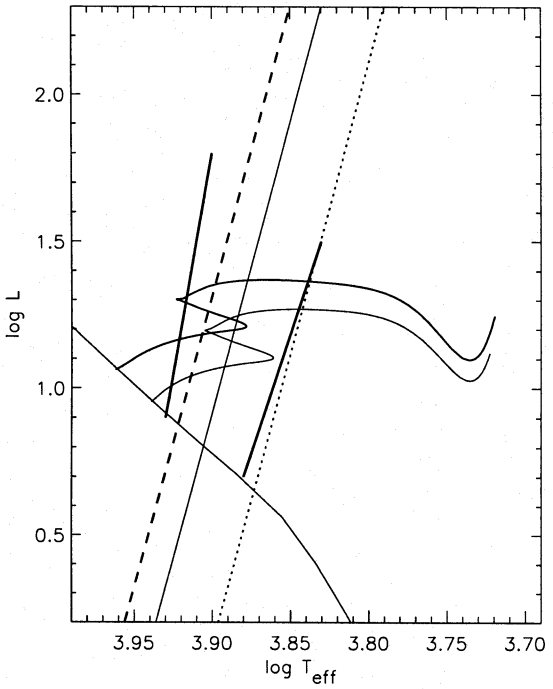

Fig. 2. The HR-diagram of our model series. The full line along the instability strip shows the position of envelope models with standard $R - L$ relation. The dotted line has $\log T_{\rm eff}$ lower than the standard sequence by -0.04, and is close to the red edge, while the dashed line has $\log T_{\rm eff}$ higher by +0.02 and is close to the blue edge. For reference ZAMS and two standard evolution tracks of mass $M = 1.6$ and $1.7\ M_\odot$ for metal content given by $Z = 0.01$ are shown. Thick lines delimit the region of the observed δ Sct stars as determined by photometry

Table 1. $M - L$ relations: $\log M = A + B\ \log L$. See text for explanation of remarks

Relation	A	B	Remark
ML1	–0.128	0.271	Standard BIT, Population I
ML2	–0.210	0.271	Modified BIT
ML3	–0.145	0.250	Simon & Kanbur, $Z = 0.02$
ML4	–0.188	0.250	Simon & Kanbur, $Z = 0.01$
ML5	–0.240	0.250	Simon & Kanbur, $Z \simeq 0.001$

& Kanbur (1994) for Cepheid models based on OPAL opacities with metal content $Z = 0.02$ and 0.01, respectively. ML5 is a similar relation with higher luminosity–to–mass ratio appropriate for classical Cepheids of very low metal content. We emphasize that in the present envelope model series we consider Z and the $M - L$ relation as completely independent parameters. These model series are particularly useful for overview purposes because they allow us to study effects from changes in Z and in the $M - L$ relation separately, while in realistic evolution models these effects are necessarily mixed up.

Fig. 1 shows the $M - L$ relations together with evolution lines for Population I models ($Z = 0.01$ and 0.02) and a Population II model ($Z = 0.001$). The models marked by squares are realistic models of AI Vel and SX Phe with the observed periods and period ratios, and are discussed in more detail later. Here we note that the AI Vel model of $Z = 0.01$ actually satisfies ML1. It is also seen that in the δ Sct region ML2 and ML4 are virtually identical and that the SX Phe model approximately satisfies these relations.

2.2. *Radius-luminosity relations*

In the HR-diagram the envelope model series are, of course, situated in the Cepheid instability strip. We use radius-luminosity relations of the form

$$\log R = C + D\ \log L\ , \qquad (2)$$

with R and L in solar units. Except where otherwise noted the radius-luminosity relation is given by $C = -0.3680$, $D = 0.6012$. This standard case in shown in Fig. 2 as a full line roughly in the middle of the instability strip. In order to check the effects of changes of the parameters C and D in the $R - L$ relation we calculate additional model series. The dashed and dotted lines show positions of such series. The dashed sequence with smaller R has $\log T_{\rm eff}$ higher than the standard sequence by +0.02 (for same $\log L$), and is situated close to the observed blue edge of the instability strip. The dotted sequence with larger R has $\Delta \log T_{\rm eff} = -0.04$, and is positioned close to the red edge of the strip (e.g. Fernie 1992; Breger 1995).

© European Southern Observatory • Provided by the NASA Astrophysics Data System

1996A&A...312..463P

2.3. Accuracy of pulsation periods and period ratios

In the following, we use both full stellar models taken from evolution sequences and standard stellar envelope models. The stellar-evolution sequences to be used in Sects. 4 and 5 for comparisons with individual stars start from chemically homogeneous static ZAMS models. The basic computations follow Christensen-Dalsgaard (1982). An accurate equation of state and OPAL opacities are used in all models. The initial hydrogen content is $X = 0.70$, except when other values are specified. Convection is treated by the mixing-length theory, with a mixing length of α pressure scale heights, the default being $\alpha = 2.0$. The envelope models use the same basic physics and defaults for α and the hydrogen abundance.

We calculate precise periods of linear, adiabatic oscillations for the fundamental mode and the first few overtones of radial oscillations (e.g. Christensen-Dalsgaard & Berthomieu 1991). When full models in evolution sequences are used, periods are computed on the complete models. Effects of rotation on the structure and oscillations of the models are neglected. We note, however, that to second order in the rotation rate even radial modes are perturbed by rotation: the relative period change can be expressed as $\delta\Pi_n^{(\mathrm{rot})}/\Pi_n = Z_n(\Pi_{\mathrm{rot}}/\Pi_n)^{-2}$, where Π_n is the unperturbed period of mode n, and Π_{rot} is the rotation period; the coefficient Z_n depends on the order of the mode and the structure of the star but is of order unity. The resulting changes in the period ratios were considered by Pérez Hernández, Claret & Belmonte (1994).

First we give an overview of the period ratios by means of series of envelope models. The present models are identical to those used by Christensen-Dalsgaard & Petersen (1995), except that we now use deeper model envelopes. The inner boundary of the models used by Christensen-Dalsgaard & Petersen had relative radius $x = r/R$ of 0.17–0.20, while the present model series typically have x less than 0.05. For the double-mode Cepheids (Π_0 larger than about 1 d) discussed by Christensen-Dalsgaard & Petersen, very small changes in the period ratios result, the largest being an increase of Π_2/Π_1 of up to +0.002 at the shortest periods.

Periods of full-amplitude oscillations of real stars differ from those given by linear, adiabatic analysis. Nonadiabatic corrections $\delta\Pi/\Pi$ are of the order of $|\eta/\omega|^2$, where η is the stability coefficient and ω is the frequency of the mode. Both nonadiabatic and nonlinear corrections are known to be very small for short periods (e.g. for δ Scuti models), but increasing for larger periods and larger L/M ratios. Kanbur (1995) has kindly calculated a series of envelope models of $Z = 0.02$ with our standard $R - L$ and ML1 relations. Kanbur's models are purely radiative, and both adiabatic and nonadiabatic periods are available for each model. In the δ Sct region ($\Pi_0 \leq 0.25$ d) nonadiabatic effects on low-order period ratios are smaller than ± 0.0002. It is also interesting to compare our adiabatic periods in models that take convection into account in the envelope structure, with the periods of Kanbur's radiative models, using otherwise the same parameters. In the δ Sct region Kanbur finds period ratios higher than ours by up to about 0.002 for modes up to the third overtone. Very similar differences are obtained if we compute instead purely radiative models. Thus the agreement is relatively good, compared with the differences in this region in Π_1/Π_0 of up to 0.015 between models based on OPAL opacities and the older Los Alamos opacities, although further tests involving independent calculations would be useful.

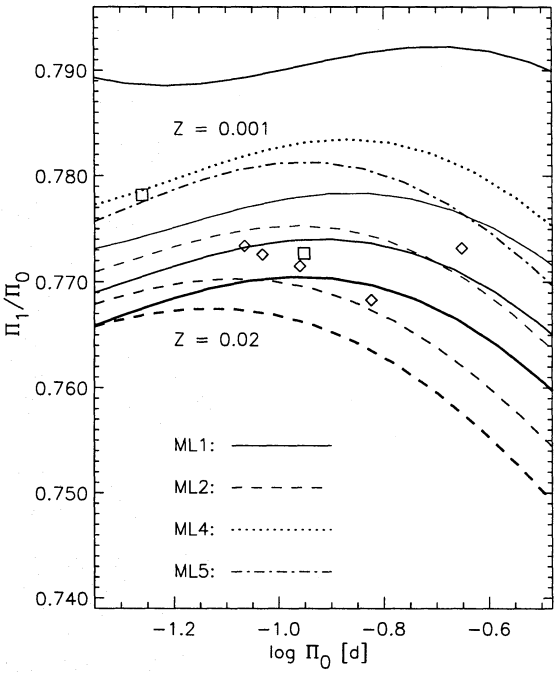

Fig. 3. Calibration of the ($\log \Pi_0$, , Π_1/Π_0) period-ratio diagram in terms of the metal content $Z = 0.02, 0.01, 0.005$ and 0.001 and four $M - L$ relations (see text for details). Observed period ratios from Table 2 for 7 double-mode δ Sct stars are shown, SX Phe and AI Vel are marked by squares, the other stars by diamonds

The uncertainties of the OPAL opacities are not known precisely. Assuming a maximum error of 10% in the present OPAL opacities, and comparing with errors in the Los Alamos opacities of up to a factor 2–3 by means of κ-effect functions (Petersen 1992), we estimate the effect on perios ratios to at most $\pm$ 0.001.

Effects of finite amplitudes on periods and period ratios are known to decrease with period for Cepheid-type models. For δ Sct models we expect very small nonlinear effects. However, this problem needs modern systematic studies.

3. The period ratios Π_1/Π_0 and Π_2/Π_1

In the following paragraphs we investigate theoretical period-ratio diagrams. In particular, we study the sensitivity of the important period ratios Π_1/Π_0 and Π_2/Π_1 to changes in a number of model parameters. In order to indicate the interesting regions of the diagrams, where the observed stars are located, we plot the known variables in some figures: the relevant data are collected in Table 2 together with additional observational quantities. However, we defer a specific discussion of individual stars to Sects. 4 and 5.

© European Southern Observatory • Provided by the NASA Astrophysics Data System

1996A&A...312..463P

Table 2. Information on high-amplitude double-mode δ Sct stars taken from McNamara (1992), if available there, or from Andreasen (1983). The data in the last three columns are semi-theoretical, based on the assumption that the stars follow standard stellar evolution theory

Star	$\log \Pi_0$ [d]	Π_1/Π_0	$T_{\rm eff}$ [K]	[Fe/H] [dex]	$M_{\rm bol}$ [mag]	$M/M_\odot$	Age [Gyr]
SX Phe	−1.260	0.7782	7850	−1.3	2.8	1.2	1.6
AE UMa	−1.065	0.7734	7500	−1	1.9	1.6	1.3
RV Ari	−1.031	0.7726	7500	−1	1.7	1.6	1.2
BP Peg	−0.960	0.7715	7470	−0.1	1.4	1.7	1.3
AI Vel	−0.952	0.7727	7620	−0.2	1.3	1.8	1.0
V703 Sco	−0.824	0.7683	7000	0	1.3	1.9	1.0
VX Hya	−0.652	0.7732	6980	0.1	0.6	2.2	0.6

3.1. Z and M − L relations: overview

Fig. 3 gives a comparison of 7 double-mode δ Sct stars identified as fundamental mode plus first overtone oscillators with our model series calculated for $Z = 0.02, 0.01, 0.005$ and 0.001. The $M-L$ relations ML1 and ML2 are illustrated for $Z = 0.02, 0.01$ and 0.005. For $Z = 0.001$ we expect a very high L/M ratio. Therefore we here use ML4 and ML5, although for comparison we also include the ML1 series with relatively low L.

It is evident that the computed period ratios show a substantial dependence on both Z and the $M - L$ relation. For $Z = 0.005 - 0.02$ and very short periods (Π_0 less than about 0.07 d) the effect on Π_1/Π_0 from the $M - L$ relation is small, and we find a separation in Π_1/Π_0 after Z. However, a change of a factor of 2 in Z only causes a change in Π_1/Π_0 of about 0.003, and we cannot exclude L/M ratios outside the ML1–ML2 interval. For $Z = 0.001$ high values of Π_1/Π_0, in the range 0.775–0.790, are obtained in the δ Sct region. However, there is a conspicuously large difference between the low-luminosity ML1 relation and the high-luminosity relations ML4 and ML5. Also, we note that the problem of the relevant $M - L$ relation for a certain star is very different for the δ Sct stars and in the Cepheid case. Low-amplitude δ Sct stars are typically main-sequence stars with $M - L$ relations far below our ML1 sequence, while most high-amplitude δ Sct stars are in the immediate post–main–sequence stage with relatively high L/M ratios, corresponding to our envelope model series.

We conclude that a period ratio alone gives little information on a particular variable star. Fig. 3 shows a systematic increase in Π_1/Π_0 with decreasing Z and decreasing L/M ratio. If Z is known, we can use the calibration curves of Fig. 3 to give information on the $M - L$ relation relevant to the star from Π_1/Π_0, or vice versa.

Of course, stellar evolution models calculated for assumed values of M and Z give the relevant value of L for each model in an evolution sequence. Normally, pulsation periods increase with evolution time due to increasing radius, and an evolution track in all period-ratio diagrams is defined. Combining information from the HR-diagram with period ratios (or ideally determination of many oscillation frequencies), detailed comparisons between observations and theoretical models can be performed. We discuss such comparisons in Sects. 4 and 5.

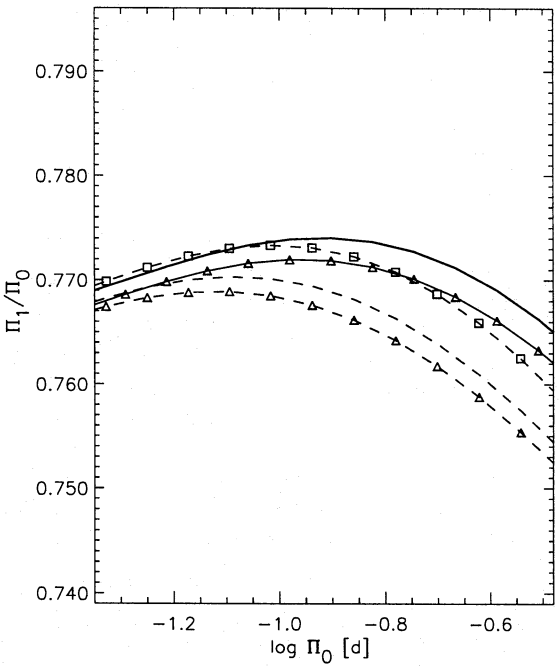

Fig. 4. Two standard model sequences with hydrogen content $X = 0.70$ are shown together with modified sequences calculated for $X = 0.75$ (marked by triangles) and one sequence of $X = 0.60$ (marked by squares). Full curves give series with $M - L$ relation ML1, dashed curves series with ML2

In the following subsections we illustrate the influence of secondary model parameters by comparing our standard model sequences having the composition $X = 0.70$, $Z = 0.01$, the standard $R-L$ relation and the default mixing-length parameter $\alpha = 2.0$ with several modified model sequences where these parameters are changed systematically.

3.2. Hydrogen content X

Standard models of formation and evolution of galaxies predict that the average helium content Y increases with increasing Z approximately according to $\Delta Y \simeq 4\ ,\Delta Z$ (e.g. Pagel 1995). Comparing stars of standard solar composition $Z = 0.02$, $X = 0.70$ with stars of lower Z, we should use $X = 0.77 - 0.75$ for

© European Southern Observatory • Provided by the NASA Astrophysics Data System

1996A&A...312..463P

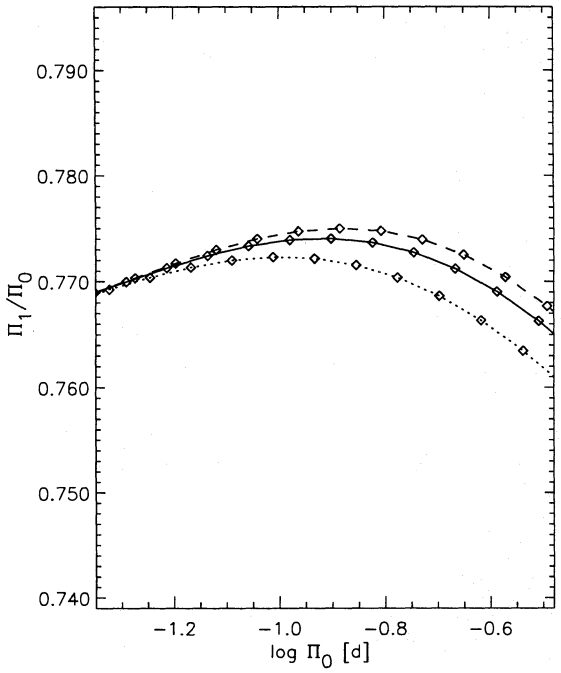

Fig. 5. The standard model sequence of $Z = 0.01$ (full curve) is given together with sequences calculated for lower R (i.e., higher $T_{\rm eff}$ for same L, dashed curve) or higher R (dotted curve). The higher R results in lower $T_{\rm eff}$ and a considerable decrease in the period ratio due to effects of changes in the envelope structure. The ML1 mass-luminosity relation is used in these series

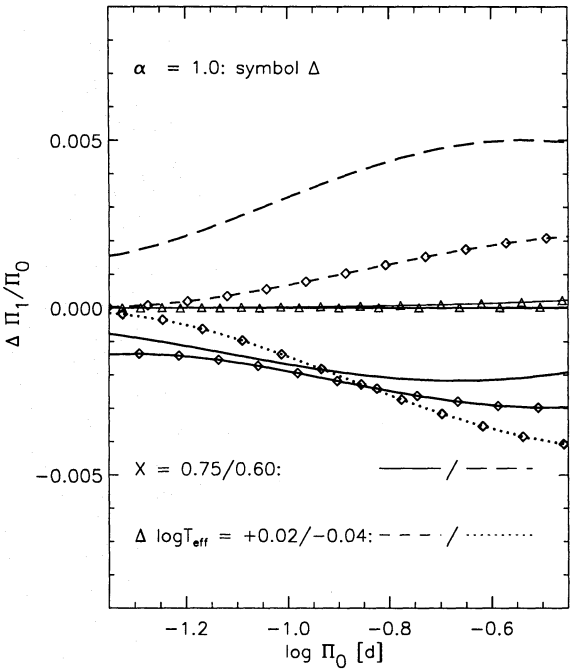

Fig. 6. Changes, at fixed Π_0, in the period ratio Π_1/Π_0 introduced by the specified changes in the secondary parameters from our standard values: hydrogen content $X = 0.70$, standard $R - L$ relation, and standard mixing-length parameter $\alpha = 2.0$. In Figs. 6 and 7 ML1 series are marked by diamonds, while ML2 series are not marked by symbols

δ Sct stars with $Z = 0.005 - 0.01$. In order to assess the effects of such a change X we compare in Fig. 4 standard model series with $X = 0.70$ with similar sequences with $X = 0.75$ and 0.60. A change of $\Delta X = +0.05$ results in a change in the period ratio of $\Delta\Pi_1/\Pi_0 = -0.001$ to -0.003. The effect of using $X = 0.60$ is to increase the period ratio by about twice this amount, as could be expected. According to standard models of galaxy evolution, stars with X significantly lower than about 0.65 will not be formed. We can therefore conclude that for δ Sct stars the uncertainty in Π_1/Π_0 introduced by a realistic uncertainty in X is less than about ± 0.002; this confirms that the hydrogen content is a secondary model parameter. A precise specification of X is only required for very precise comparisons with observed period ratios.

3.3. R – L relations and effective temperature

Fig. 5 compares the ML1 model sequence for $Z = 0.01$ and standard radius-luminosity relation with two sequences with smaller/larger R (for same L, cf. Fig. 2). The dashed sequence with smaller R has $\log T_{\rm eff}$ higher than the standard sequence by +0.02, while the dotted sequence with larger R has $\Delta \log T_{\rm eff} = -0.04$. The dashed sequence gives increased Π_1/Π_0 by up to about +0.0025, whereas the dotted sequence shows a considerable decrease in the period ratio (by up to about −0.004). A separate calculation has shown that rather similar results are obtained from purely radiative models, although the effect with decreasing $T_{\rm eff}$ is somewhat larger. Thus the changes in period ratios are apparently not related to effects of convection on the structure of the equilibrium model.

We conclude that for models in the low-$T_{\rm eff}$ part of the Cepheid instability strip calibration curves may depend sensitively on the precise position of the model within the strip. In the high-$T_{\rm eff}$ part of the strip the assumed $R - L$ relation is a secondary parameter, and at typical δ Sct periods of about 0.1 d this effect is always small.

3.4. Mixing length α

In order to check effects on the period ratio from changes in α, we consider two series with mixing-length parameter $\alpha = 1.0$ instead of the default $\alpha = 2.0$, i.e., with less efficient convection. The modified sequences are almost identical to the standard sequences (see also Fig. 6). This is true also close to the red edge of the instability strip in the δ Sct region. We conclude that for otherwise identical models the precise value of the mixing-length parameter has very little influence in the δ Sct region.

3.5. Sensitivity of Π_1/Π_0 to secondary parameters

In Fig. 6 we plot the *changes* in the period ratio Π_1/Π_0 due to the changes in the secondary parameters from our standard values just described in the subsections above. Results for two mass-luminosity relations are illustrated: here and in Fig. 7 the

© European Southern Observatory • Provided by the NASA Astrophysics Data System

1996A&A...312..463P

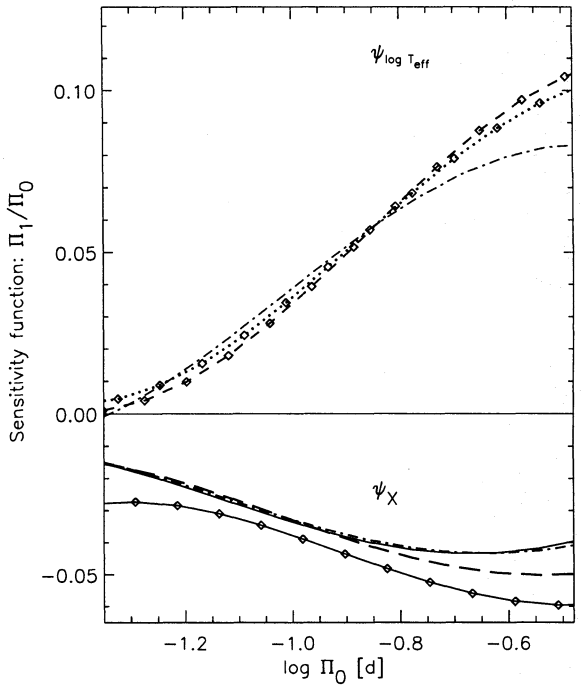

Fig. 7. Sensitivity functions giving the sensitivity of the period ratio Π_1/Π_0 to changes in the secondary parameters hydrogen content X and effective temperature $\log T_{\rm eff}$. Series with $(X,\ Z) = (0.70,\ 0.01)$ and mass-luminosity relations ML1 (marked by a diamond) or ML2 (no marks) are modified. Most series are taken over from Fig. 6 with the same coding. Two additional series with very small parameter changes ($\Delta X = 0.01$ or $\Delta \log T_{\rm eff} = -0.005$) are shown by dot-dashed curves

ML1 series are marked by diamonds, while the ML2 series are not marked by symbols.

Given that $X = 0.60$ is an unrealistic value, realistic uncertainties in X (of ± 0.05) are seen to result in uncertainties in the period ratio of less than about ± 0.002. We also note that comparison of the curves for $X = 0.60$ (i.e., a deviation of $\Delta X = -0.10$ from our standard value of $X = 0.70$) and $X = 0.75$ ($\Delta X = +0.05$) shows that $\Delta[\Pi_1/\Pi_0]$, $(\log \Pi_0)$ for $\Delta X = -0.10$ is of opposite sign to and approximately twice the numerical value of the changes for $\Delta X = +0.05$.

The effects of changing $T_{\rm eff}$ are illustrated for the ML1 sequence by the short-dashed and dotted curves in Fig. 6. In the whole period interval, the effect of $\Delta \log T_{\rm eff} = -0.04$ is of the opposite sign to and about twice as large as the effect of $\Delta \log T_{\rm eff} = +0.02$. Thus, as for the change in X, we find that the change in Π_1/Π_0 varies almost linearly with the change in the parameter.

We finally find that changing α from 2 (our standard) to 1 changes Π_1/Π_0 by less than 2×10^{-4} in δ Sct models.

From these results we conclude that the influence of the secondary model parameters results in uncertainties $\Delta[\Pi_1/\Pi_0]$ of less than about ± 0.002, apart from the effects of large changes in X or substantial changes in $T_{\rm eff}$ near the red edge of the instability strip.

3.6. Sensitivity functions

Except in special cases the changes in the models, and hence in the periods and period ratios, can be approximated by linear functions of the changes in the parameters, for sufficiently small changes. For any parameter ζ we can therefore introduce a *sensitivity function* ψ_ζ for the period ratio Π_1/Π_0 to changes in that parameter, as

$$\psi_\zeta \equiv \frac{\partial(\Pi_1/\Pi_0)}{\partial \zeta} \ ; \tag{3}$$

specifically, the derivative is taken at fixed fundamental period Π_0, corresponding to the observational constraints, by varying L and hence M and R along the relevant $M - L$ and $R - L$ relations; all other model parameters are kept fixed. Given a sequence of models, this can be regarded as a function $\psi_\zeta(\log \Pi_0)$ of Π_0. We note that ψ_ζ is similar to the *κ-effect function* introduced by Petersen (1992) and Christensen-Dalsgaard (1993) to describe the response of the period ratios to changes in the opacity.

In practice, we have estimated the sensitivity functions as

$$\psi_\zeta = \frac{\partial(\Pi_1/\Pi_0)}{\partial \zeta} \simeq \frac{\delta(\Pi_1/\Pi_0)}{\delta \zeta} \ , \tag{4}$$

where $\delta\zeta$ is a chosen test change and $\delta(\Pi_1/\Pi_0)$ is the resulting change in the period ratio, the difference being evaluated at fixed Π_0. By varying $\delta\zeta$, we can evidently test the assumed linearity. We note, however, that more systematic calculations of the response of models and frequencies to parameter changes can be based on linearizing the equations of stellar structure and the variational principle for the oscillation frequencies (e.g. Gough & Kosovichev 1990; see also Balmforth et al. 1995).

The differences presented in Fig. 6 have been used to obtain the estimates of the sensitivity functions ψ_X and $\psi_{\log T_{\rm eff}}$ to changes in the hydrogen abundance and effective temperature shown in Fig. 7, with the addition of two cases using very small parameter changes (dot-dashed curves). We have already noted that $\Delta(\Pi_1/\Pi_0)$ scales approximately as ΔX. In accordance with this, the estimates of ψ_X for the model sequences using ML2 are largely independent of ΔX, except for $\Delta X = -0.10$ and the longest periods. We conclude that our results provide a well-defined estimate of ψ_X. It is interesting, however, that ψ_X shows considerable dependence on the choice of mass-luminosity relation, as indicated by the curve marked by diamonds: for ML1 the sensitivity seems to be substantially larger than for ML2, particularly at very short and at long periods.

In the case of $T_{\rm eff}$, Fig. 7 shows that the assumption of linearity is very well satisfied; also, the sensitivity function depends little on the mass-luminosity relation except for the longest periods, where we find a difference of about 20% between results based on ML1 and ML2. We conclude that our model sequences provide reasonably robust estimates of the sensitivity function.

3.7. Systematic parameter estimation

The general problem of constraining stellar model parameters from observed quantities was discussed by Brown et al. (1994).

© European Southern Observatory • Provided by the NASA Astrophysics Data System

1996A&A...312..463P

They considered the task of improving a good guess of the true parameter set, through a linear least-squares fit of the parameters to a set of observed quantities. This process requires values of all partial derivatives $\partial B_i/\partial P_j$, where B_i is the set of observables and P_j is the set of parameters [see Eq. (3) of Brown et al.]. Here we consider the accurately known observable Π_1/Π_0, assuming that models are selected with a specific value of the period Π_0, and base the analysis on envelope models; the relevant parameters are then Z, the $M-L$ relation, X, the $R-L$ relation and α. Evidently, more observables, e.g. independent constraints on the heavy-element abundance and effective temperature, would be required in actual applications of the fitting procedure. The condition for the procedure to work properly is that all derivatives $\partial B_i/\partial P_j$ are well defined. In our case the relevant derivatives are represented by the sensitivity functions, e.g. ψ_X and $\psi_{\log T_{\rm eff}}$, which therefore must have unique values at each Π_0. In normal, non-singular models this will be the case.

Fig. 7 shows that the relevant sensitivity functions are indeed comparatively well defined for the δ Sct models; for example, ψ_X is determined to within about 30% at a fixed period. However, the dependence of ψ_X on the $M-L$ relation indicates that the parameters cannot be determined independently. We note that the parameter improvement process can often work satisfactorily with approximate values of the partial derivatives, although more iterations may then be needed.

Good approximations to the partial derivatives needed in the iterative parameter improvement can be obtained by using very small test changes δ in the parameters. Examples are shown in Fig. 7. There is comparatively close agreement in most of the relevant period interval between the resulting curves and those obtained with parameter changes which are substantial fractions of the full parameter interval within the instability strip. This fact indicates that the systematic parameter improvement process can be used successfully, using a relatively small number of model envelope series.

3.8. *The period ratio* Π_2/Π_1

We have studied the period ratio Π_2/Π_1 in the same way as Π_1/Π_0. A comparison of the calibration of the ($\log\Pi_1$, , Π_2/Π_1) period-ratio diagram by model series calculated for Z = 0.02, 0.01, 0.005 and 0.001 with Fig 3 shows that the main properties of these calibration diagrams are remarkably similar; details are not given here. The sensitivity of Π_2/Π_1 to secondary parameters is also found to be similar to the the sensitivity of Π_1/Π_0, which has just been described. We here only note that at typical δ Sct star periods of about 0.1 d the changes in secondary parameters result in changes in Π_2/Π_1 of less than about $\pm$ 0.0015.

4. SX Phoenicis

SX Phe is important for several reasons. It is the only known Population II double-mode high-amplitude field δ Sct star, and by good luck it is so close that an accurate HIPPARCOS parallax can be expected in 1996. With the OPAL opacities the observed period ratio gives a strong constraint on the models which, together with the accurate parallax, will provide a stringent model test. Therefore we study SX Phe in some detail using both envelope models and evolution sequences.

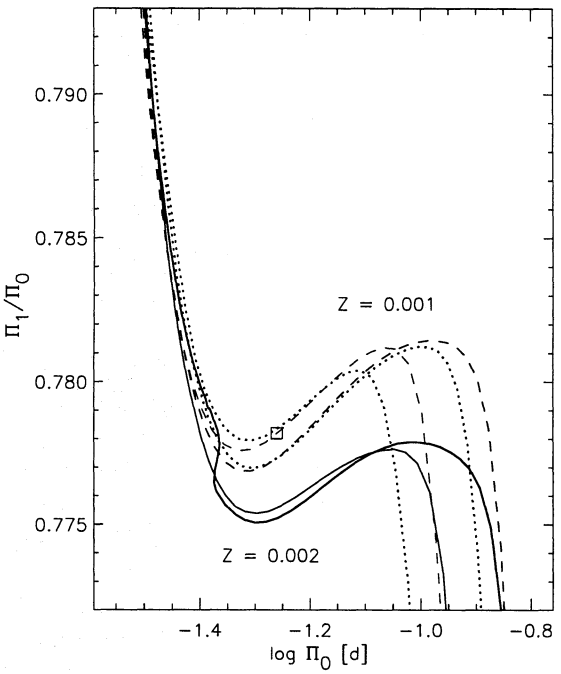

Fig. 8. Comparison of standard evolution tracks in the period-ratio diagram with SX Phe [□]. Full curves give tracks calculated for (X, , Z) = (0.70, , 0.002) of mass 1.1 and 1.2 $M_\odot$. Dashed curves are for (X, , Z) = (0.70, , 0.001) and mass 1.0 and 1.1 $M_\odot$, and dotted curves for (X, , Z) = (0.75, , 0.001) and mass 1.0 and 1.1 $M_\odot$. SX Phe agrees perfectly with two models both of mass 1.0 $M_\odot$

We can now use the accurately known period ratio Π_1/Π_0 = 0.7782 (Π_0 = 0.0550 d) of SX Phe in precise modelling. Determinations of metal content and other observational quantities of SX Phe scatter considerably (e.g. Nemec & Mateo 1990, Table 1). The most recent [Fe/H] is −1.3 (cf. Table 2) or $Z \simeq 0.001$. Fig. 3 shows that this value of Z gives the observed Π_1/Π_0 for ML4.

Figs. 8 and 9 give comparisons of observations of SX Phe taken from Table 2 with standard evolution model sequences in the period-ratio and HR-diagrams. Fig. 8 shows that the observed Π_1/Π_0 agrees with evolution models of Z = 0.001 within $\pm$ 0.001, while Z = 0.002 predicts $\Pi_1/\Pi_0 \simeq 0.7755$, far below the observed value. The models that agree perfectly with SX Phe both have mass 1.0 $M_\odot$.

Fig. 9 shows an HR-diagram containing the same evolution sequences as Fig. 8 with identical coding, and the position of SX Phe according to Table 2 marked by a square. The luminosity ($M_{\rm bol}$) in Table 2 is not based on a directly observed distance. Rather, this value is estimated from the *assumption* that SX Phe follows standard evolution. Therefore we cannot check this assumption by means of Fig. 9. The observational constraints on

© European Southern Observatory • Provided by the NASA Astrophysics Data System

1996A&A...312..463P

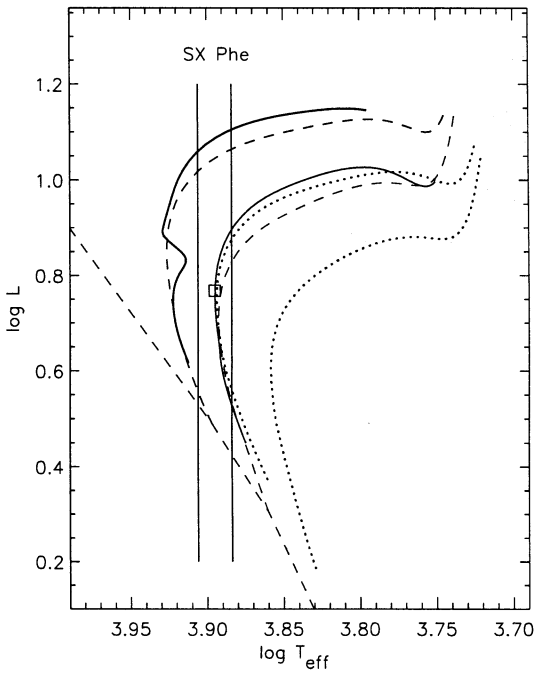

Fig. 9. HR-diagram showing a comparison of standard evolution tracks with SX Phe [□]. The coding giving the parameters of model sequences is precisely the same as in Fig. 8. Observations ($T_{\rm eff}$) constrain the position of SX Phe to be between the vertical lines. The luminosity is not known directly from presently available observations

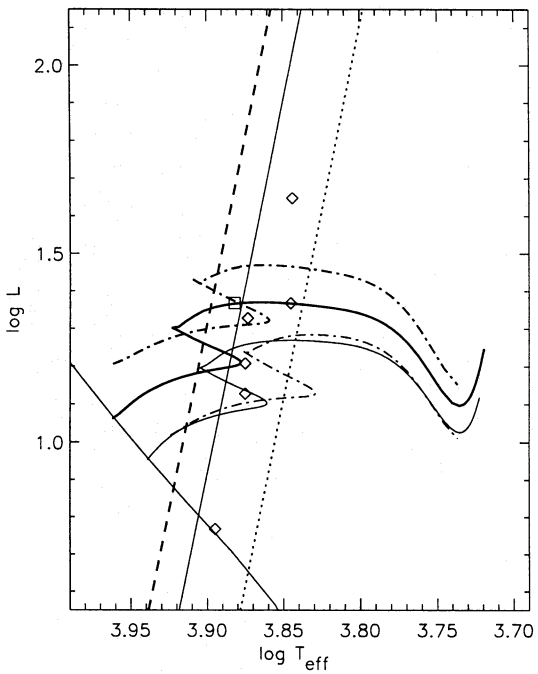

Fig. 10. HR-diagram showing a comparison of standard evolution tracks calculated for $Z = 0.01$ (full curves) and $Z = 0.02$ (dash-dotted curves) with AI Vel [□] and other stars from Table 2 [◇]. Masses are 1.6 and 1.7 $M_\odot$ for $Z = 0.01$ and 1.8 and 2.0 $M_\odot$ for $Z = 0.02$. The instability strip is roughly indicated as in Fig. 2. It is seen that most high-amplitude stars are located close to our standard $R - L$ relation, justifying this choice for envelope models

SX Phe are given by the vertical lines, which mark the observed $T_{\rm eff} = (7850 \pm 200)$ K.

From Figs. 8 and 9 it is seen that only one model of SX Phe satisfies the observational constraints in both the period ratio and the HR-diagram, namely the model with $X = 0.70$, $Z = 0.001$, $M = 1.0\ M_\odot$ and the observed period $\Pi_0 = 0.0550$ d. This model has $T_{\rm eff} = 7684$ K, $\log L = 0.82$ ($M_{\rm bol} = 2.68$) and age = 4.07 Gyr. We estimate somewhat lower luminosity and mass, and consequently larger age, than did McNamara (1992) and Kim et al. (1993), because they used models with a higher $Z = 0.0017$.

Comparing evolution models calculated for $Z = 0.0005$ with the SX Phe data, we find that this value of Z does not allow an acceptable solution, although we can obtain the observed period ratio in models of mass 1.1–1.2 $M_\odot$. However, models with the observed Π_0 and a period ratio close to the observed value have too high $T_{\rm eff}$ and L. Also, we note that $Z = 0.0005$ corresponds to an [Fe/H] which is much lower than the observed value of –1.3 to –1.0.

Using the observed V magnitude of 7.28 mag (Rodríguez et al. 1994) and a bolometric correction of $BC = -0.02$ mag, the above $M_{\rm bol}$ gives a distance to SX Phe of 82 parsec or a parallax of 0.012 arcsec. It is difficult to estimate an uncertainty is this parallax, both because we do not know the uncertainties of the OPAL opacities, and because the observational data on SX Phe published in the literature scatter considerably. However, if we rely on the OPAL opacities, require agreement with the observed period ratio within ± 0.001, and agreement in $T_{\rm eff}$ within ± 200 K, we can estimate an uncertainty of the parallax of about ± 0.002 arcsec. This result

$$\pi = 0.012 \pm 0.002 \text{ arcsec}\ , \qquad (5)$$

gives an interesting prediction of the HIPPARCOS parallax to be published in the Spring of 1996. The HIPPARCOS Input Catalogue gives $\pi = 0.023 \pm 0.008$ arcsec for SX Phe, and the General Catalogue has $\pi = 0.026 \pm 0.007$ arcsec (Jenkins 1957).

5. AI Velorum and other Population I stars

5.1. The Population I group

In Fig. 10 we give an HR-diagram comparing standard evolution tracks for $Z = 0.01$ and 0.02 with data taken from Table 2, and Fig. 11 gives the same comparison in the period-ratio diagram with identical coding. These figures show that the assumption that the high-amplitude δ Sct variables follow standard stellar evolution gives a natural explanation of the observed HR- and period-ratio diagrams. This is not a new conclusion. However, the application of OPAL opacities now provides an improved check. We can now trust theoretical period ratios within about ± 0.001 – a factor of about 10 better than before 1992. When more accurate [Fe/H] and the HIPPARCOS parallaxes become available, it will be interesting to discuss all stars of the Population I group individually.

© European Southern Observatory • Provided by the NASA Astrophysics Data System

1996A&A...312..463P

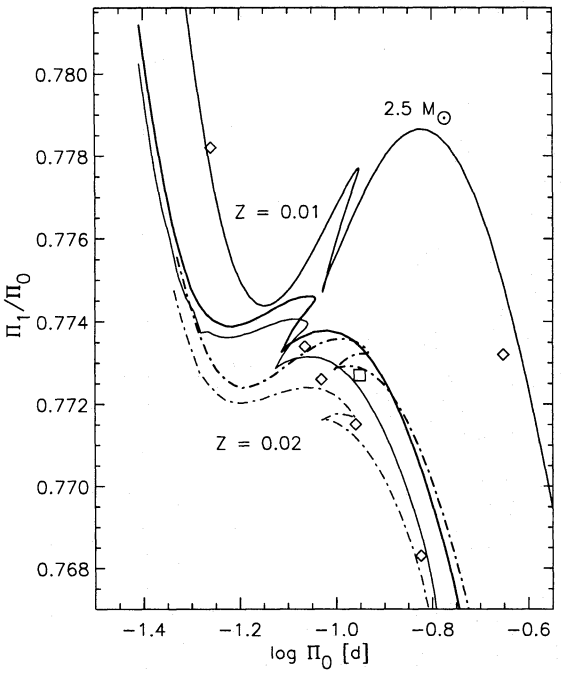

Fig. 11. Period ratio diagram showing a comparison of standard evolution tracks calculated for $Z = 0.01$ and $Z = 0.02$ with the stars from Table 2. Coding is identical with that of Fig. 10. Here a model sequence of mass 2.5 $M_\odot$ is also included

5.2. AI Velorum

Walraven et al. (1992) determined five oscillation frequencies in AI Vel. Those of high amplitude are the well-known fundamental and first-overtone radial modes given here in Table 2, and Walraven et al. propose a tentative identification of two additional frequencies in terms of the third and fifth radial overtone. A fifth mode, intermediate in period between the fundamental and first overtone must be a nonradial mode. This makes AI Vel a very interesting object for asteroseismology. Here we start by analysing AI Vel in the same way as we just considered SX Phe.

According to McNamara (1992, cf. Table 2) [Fe/H] of AI Vel is −0.2, i.e., $Z \simeq 0.01$. We first note that AI Vel in Fig. 10 is located precisely on the 1.7 $M_\odot$ track for $Z = 0.01$ in the post–main–sequence (PMS) evolution stage. However, here again the luminosity is not a directly empirically determined quantity, so that Fig. 10 gives only a weak constraint on the model. In Fig. 11 it is seen that AI Vel for $Z = 0.01$ is found in the PMS stage between the tracks of mass 1.6 and 1.7 $M_\odot$. The best solution is $M \simeq 1.62 M_\odot$. This solution is the same as the solutions preferred by McNamara (1992) and Andreasen (1983). Now we have agreement with the observed period ratio thanks to the OPAL opacities, in contrast to earlier studies. For a chosen/observed Z, Π_1/Π_0 allows us to give a very precise solution. Again we caution that although application of OPAL opacities clearly gives a significant improvement over older opacities, we do not know the effects of the remaining uncertainties on the period ratios.

Since the observed metal content is usually rather uncertain, it is of interest to consider briefly solutions for other assumed Z-values. Therefore we have included also tracks of $Z = 0.02$ in Figs. 10 and 11. To some surprise we find from Fig. 11 that $M = 2.0\,, M_\odot$ here also gives a good solution in the PMS stage for the period ratio. Recalling that the observations give reliable values of $T_{\rm eff}$ but not of L, Fig. 10 shows that this solution is also acceptable.

Fig. 11 shows that in the post–main–sequence stage it is possible to cover the same region in the Π_1/Π_0 diagram with realistic models both of $Z = 0.01$ and $Z = 0.02$. This can be understood from the fact that Π_1/Π_0 depends both on Z and the $M - L$ relation (Sect 3). A change in Z from 0.01 to 0.02 will decrease Π_1/Π_0 (Fig. 3). However, for $Z = 0.02$ the relevant $M - L$ relation is less luminous, as illustrated in Fig. 1. According to Fig. 3 this will again increase Π_1/Π_0. This compensating effect is probably responsible for the remarkably narrow interval $\Pi_1/\Pi_0 = 0.771 \pm 0.002$ found among the Population I high-amplitude δ Sct stars.

Our preferred model of AI Vel with $Z = 0.01$ and $M = 1.62\,, M_\odot$ has $M_{\rm bol} = 1.51$. With the observed $V = 6.70$ and $BC = -0.02$, this leads to a predicted parallax of 0.009 arcsec. The model with $Z = 0.02$ and $M = 2.0\,, M_\odot$ similarly predicts a parallax of 0.007 arcsec. The HIPPARCOS Input Catalogue for AI Vel gives $\pi = 0.028 \pm 0.011$ arcsec; thus, as in the case of SX Phe, we obtain a parallax smaller than the previously determined trigonometric value.

5.3. Low-amplitude modes

As mentioned above, Walraven et al. (1992) found three additional low-amplitude modes excited in AI Vel, of which one must be nonradial. They proposed identification of two modes with the radial third and fifth overtones with observed period ratios of $\Pi_3/\Pi_0 = 0.5280$ and $\Pi_5/\Pi_0 = 0.3979$. We can compare these values with theoretical period ratios in AI Vel models with the observed fundamental period and period ratio Π_1/Π_0, using both the evolution tracks described above and the envelope model sequences. In all cases we find that both the theoretical Π_3/Π_0 and Π_5/Π_0 are too small by an amount of 0.01–0.02. This is a large error, considering that we expect the theoretical period ratios to be accurate within ± 0.001. We have also shown that changes in the secondary model parameters do not improve the situation. We conclude that these two low-amplitude modes in AI Vel cannot be explained as radial modes in our models. Although we cannot completely rule out substantial effects of additional errors in the models, it seems most likely that the low-amplitude modes are nonradial. This possibility should be studied in detail, but is outside the scope of the present investigation. Because the frequency spectrum of nonradial modes in δ Sct stars is so rich and complicated (e.g. Dziembowski & Królikowska 1990; Breger 1995; Frandsen et al. 1995), it then becomes much more difficult to give a safe mode identification. On the other hand, given the fairly well-defined model and safe identification of the two high-amplitude oscillations, AI Vel rep-

© European Southern Observatory • Provided by the NASA Astrophysics Data System

1996A&A...312..463P

resents an interesting possibility for reliable mode identification of low-amplitude modes in δ Sct stars.

6. Discussion and conclusion

Based on our results we may consider the important problem of the possible basic differences between normal low-amplitude δ Sct stars and the high-amplitude group.

Figs. 10 and 11 indicate that all known double-mode δ Sct stars are situated in the central part of the instability strip and probably belong to the post–main–sequence evolution stage. We propose that these conditions are necessary for a star to appear as a high-amplitude variable. This can explain the much higher abundance of low-amplitude than of high-amplitude δ Sct stars: the duration of the post–main–sequence phase within the instability strip is only a small fraction of the main-sequence life-time. As far as we know, only low-amplitude δ Sct stars are known in open clusters. This may be due to the small number of δ Sct stars currently detected in open clusters. However, as more and more such δ Sct stars are discovered, it seems likely that a cluster will be found with at least one high-amplitude variable (possibly in the PMS evolution stage), allowing a more direct comparison of low- and high-amplitude stars in identical surroundings.

Very recently, two detailed studies of low-amplitude δ Sct stars using comparisons of theoretical models and observations in the HR-diagram in combination with analysis of several oscillation frequencies in the same way as our study of AI Vel, have been published. Frandsen et al. (1995) identified four modes of amplitude 3–6 mmag in the δ Sct star κ^2 Bootis. They succeeded in constructing a standard model close to the end of the MS evolution stage, which fits everything well, but with an unlikely combination of modes. They concluded that unique and safe identification of modes in such stars is probably not possible without additional constraints provided by observations of e.g. phase delays. In the HR-diagram their model is situated in the blue part of the instability strip precisely on the dashed line of our Fig. 10 with $T_{\rm eff}$ about 500 K higher than that of the high-amplitude variables. Breger et al. (1995) used very extensive data for FG Virginis to determine frequencies of 10 modes, of which one had an amplitude of 22.4 mmag and the remaining 9 had amplitudes of 1–4.4 mmag. They proposed a preliminary identification of these frequencies in a model with 1.8 $M_\odot$ in the advanced MS stage. However, they pointed out that both the stellar model adopted and the mode identification must be regarded as preliminary, and that alternative identifications should be considered as well. Their data give a position in the central part of the HR-diagram precisely where the high-amplitude variables are also located. Christensen-Dalsgaard et al. (1995) discussed solar-like oscillations in η Bootis. Their preferred models are remarkably similar to our AI Vel model with respect to evolution stage (PMS) and mass ($\simeq$ 1.65 $M_\odot$). They have, however, $Z \simeq 0.03$ and somewhat lower $T_{\rm eff}$ than δ Sct stars, which is expected for solar-like oscillators.

These three examples of low-amplitude oscillators, which seem to be normal stars in the PMS evolution stage, appearing in approximately the same region of the HR-diagram as the high-amplitude δ Sct stars, illustrate that in this group the main difficulty for very precise testing of the theoretical stellar models is to achieve safe mode identification. Needless to say, the physical mechanisms distinguishing between low- and high-amplitude variables amongst the δ Sct stars and selecting the modes that are excited to observable amplitudes are also of great interest. In studies of the mode-selection mechanism stars like AI Vel with both high- and low-amplitude modes may be especially useful.

Pérez Hernández et al. (1994) presented an analysis of observed frequencies of the LADS stars BN and BU Cancri, with 5 respectively 6 measured frequencies. They identified the stars as being on the main sequence. As an aid to mode identification, they considered period ratios for suitably selected pairs of modes; by comparing with the relatively stable ratios between periods of radial modes they identified those amongst the modes which are likely to be radial, and furthermore obtained constraints on the parameters of the stellar model. Given these identifications, they made tentative identifications of the remaining frequencies in terms of nonradial modes. They also considered the effects of rotation which, from observed values of the projected rotational velocity $V \sin i$, is known to be comparatively rapid for these two stars. This study clearly emphasized the importance of independent information about rotation, particularly in analysis of complex spectra of potentially nonradial modes.

Important information on the nature of the high-amplitude group can be expected from analysis of high-amplitude stars in globular clusters. Since they seem to have masses considerably larger than masses at the cluster turn-off from the main-sequence, they probably have been produced by mass-transfer in binary systems or even by coalescence as blue stragglers (e.g. Stryker 1993). Very recently, Gilliland et al. (1995) discovered several high-amplitude δ Sct stars in the central region of 47 Tucanae. They give pulsation periods of a star with Π_0 = 0.1020 d and Π_1/Π_0 = 0.7724, almost identical with those of AI Vel. Since 47 Tuc is a relatively metal-rich globular cluster, it is perhaps not surprising that this star has a period ratio as the Population I field stars rather than the much higher value expected for Population II SX Phe variables. When the metal content and other physical properties of the 47 Tuc sample have been determined, comparisons with the field variables will be very interesting.

Acknowledgements. We thank Shashi Kanbur for unpublished results of pulsation calculations and G.K. Andreasen, H. Schnedler Nielsen and an anonymous referee for comments on the manuscript. This work was supported in part by the Danish National Research Foundation through its establishment of the Theoretical Astrophysics Center.

References

Andreasen, G.K. 1983, A&A, 121, 250
Andreasen, G.K., Petersen, J.O. 1988, A&A, 192, L4
Baglin, A., Breger, M., Chevalier, C. et al. 1973, A&A, 23, 221

© European Southern Observatory • Provided by the NASA Astrophysics Data System

1996A&A...312..463P

Balmforth, N.J., Gough, D.O., Merryfield, W.J., 1995, MNRAS, in press
Becker, S.A., Iben, I., Tuggle, R.S. 1977, ApJ, 218, 633
Breger, M. 1979, PASP, 91, 5
Breger, M. 1980, ApJ, 235, 153
Breger, M. 1990, in "Confrontation between stellar pulsation and evolution", eds C. Cacciari, G. Clementini, ASP Conf. Ser., 11, 263
Breger, M. 1995, in "GONG '94: Helio- and Astero-Seismology", ASP Conf. Ser., 76, 596
Breger, M., Handler, G., Nather, R.E. et al. 1995, A&A, 297, 473
Brown, T.M., Christensen-Dalsgaard, J., Weibel-Mihalas, B., Gilliland, R.L. 1994, ApJ, 427, 1013
Chiosi, C., Wood, P.R., Capitano, N. 1993, ApJS, 86, 541
Christensen-Dalsgaard, J. 1982, MNRAS, 199, 735
Christensen-Dalsgaard, J. 1993, in "Inside the Stars", IAU Coll. 137, eds W.W. Weiss, A. Baglin, ASP Conf. Ser., 40, 483
Christensen-Dalsgaard, J., Bedding, T.R., Kjeldsen, H. 1995, ApJ, 443, L29
Christensen-Dalsgaard, J., Berthomieu, G. 1991, in "Solar interior and atmosphere", eds A.N. Cox, W.C. Livingston, M. Matthews, Univ. Arizona Press, p. 401
Christensen-Dalsgaard, J., Petersen, J.O. 1995, A&A, 299, L17
Dziembowski, W., Kozłowski, M. 1974, Acta Astron., 24, 245
Dziembowski, W., Królikowska, M. 1990, Acta Astron., 40, 19
Fernie, J.D. 1992, AJ, 103, 1647
Fernley, J., Jameson, R.F., Sherrington, M.R., Skillen, I. 1987, MNRAS, 208, 853
Frandsen, S., Jones, A., Kjeldsen, H. et al. 1995, A&A, 301, 123
Frandsen, S., Kjeldsen, H. 1990, in "Confrontation between stellar pulsation and evolution", eds C. Cacciari, G. Clementini, ASP Conf. Ser., 11, 312
Gilliland, R.L., Edmonds, P.D., Petro, L. et al. 1995, ApJ, 447, 191
Gough, D.O., Kosovichev, A.G. 1990, in "Proc. IAU Colloquium No 121, Inside the Sun", eds G. Berthomieu, M. Cribier, Kluwer, Dordrecht, 327
Iglesias, C.A., Rogers, F.J., Wilson, B.G. 1992, ApJ, 397, 717
Jenkins, S.L. 1957, General Catalogue of Trigonometric Stellar Parallaxes, Yale Univ. Obs.
Kanbur, S.M. 1995, private communication
Kim, C., McNamara, D.H., Christensen, C.G. 1993, AJ, 106, 2493
McNamara, D.H. 1992, "Stars, Cepheid Variable, Dwarf", in "The Astronomy and Astrophysics Encyclopedia", ed. S.P. Maran, Cambridge Univ. Press, Cambridge, p. 720
Moskalik, P., Buchler, J.R., Marom, A. 1992, ApJ, 385, 685
Nemec, J., Mateo, M. 1990, in "Confrontation between stellar pulsation and evolution", eds C. Cacciari, G. Clementini, ASP Conf. Ser., 11, 64
Pagel, B.E.J. 1995, in "Astronomical and Astrophysical Objectives of Sub-milliarcsecond Optical Astrometry", eds E. Høg, P.K. Seidelmann, Kluwer Publ., Dordrecht, Holland, p. 181
Pérez Hernández, F., Claret, A., Belmonte, J. A., 1994, A&A, 295, 113
Petersen, J.O. 1976, in "Multiple Periodic Variable Stars", IAU Coll. 29, ed W.S. Fitch, Budapest, p. 195
Petersen, J.O. 1992, A&A, 265, 555
Rodríguez, E., Lopez de Coca, P., Rolland, A. et al. 1994, A&AS 106, 21
Rodríguez, E., Lopez de Coca, P., Costa, V., Martin, S. 1995, A&A, 299, 108
Simon, N.R., Kanbur, S.M. 1994, ApJ, 429, 772
Stryker, L.L. 1993, PASP, 105, 1081
Walraven, Th., Walraven, J., Balona, L.A., 1992, MNRAS, 254, 59

This article was processed by the author using Springer-Verlag LaTeX A&A style file *L-AA* version 3.

© European Southern Observatory • Provided by the NASA Astrophysics Data System